






Article

A General Design Procedure for Symmetrical Windings of Electrical Machines

Massimo Caruso ^{1,*} , Antonino Oscar Di Tommaso ¹ , Fabrizio Marignetti ² , Rosario Miceli ¹  and Giuseppe Ricco Galluzzo ¹ 

¹ Department of Energy, Information Engineering and Mathematical Models (DEIM), University of Palermo, viale delle Scienze, Building nr. 9, 90128, Palermo, Italy.

² Department of Electrical and Information Engineering (DIEI), University of Cassino and South Lazio, via G. Di Biasio, 43, 03043, Cassino, Italy.

* Corresponding author: Antonino Oscar Di Tommaso, e-mail: antoninooscar.ditommaso@unipa.it

Academic Editor: name

Version January 25, 2018 submitted to

Abstract: Winding design methods have been a subject of research for many years of the past century. Many methods have been developed, each one characterized by some advantages and some drawbacks. Nowadays, the star of slots is the most widespread design tool for electrical machine windings. In this context, this paper presents a simple and effective procedure to determine the distribution of the EMF stars and of the winding configuration in all possible typologies of electrical machines equipped with symmetrical windings. Moreover, this procedure can also be easily implemented in a computer program in order to perform automated winding designs for rotating electrical machines. Several examples are provided in order to validate the proposed procedure.

Keywords: Rotating electrical machines; winding design; symmetrical winding; star of slots.

Nomenclature

N	nr. of slots;
m	nr. of phases;
p	nr. of pole pairs;
γ	nr. of wound coils per phase;
i	nr. of winding layers;
η	nr. of empty slots;
q	nr. of wound slots per pole per phase;
t	greatest common divider between N and p ;
y_c	coil pitch;
\mathbb{N}	the set of natural numbers;
\mathbb{G}	the set of even numbers;
\mathbb{U}	the set of odd numbers.

1. Introduction

Over the last century, several procedures for the design of the windings of electrical machines have been proposed in the literature. The first studies on the synthesis of windings date back to the first decade of the 20th century and can be attributed to E. Arnold, R. Richter and W. Kauders. The first proposed a systematic method based on the so-called star of slots (the original German term was *Nutenstern*) to solve design issues on windings of both AC and DC machines [1,2], whereas the second author improved these techniques particularly for AC machines [3]. In the same period W. Kauders, who changed his name in W. Klima after 1945, developed a study of two and three-phase windings, also providing general formulas to determine the winding factors [4,5]. In the 1950's Richter completed his researches and published a book concerning this topic [6]. Thus, it can be stated that a wide part of the literature regarding the winding design was accomplished in Europe mainly by German researchers

from late 1890 to early 1960's and many of these works were collected in a three-volumes book, written by the Austrian H. Sequenz [7–9]. In the same time, French researchers, such as H. de Pistoye [10], followed by German-Czechoslovakians [5,11], Italians [12], Japanese [13] and American scholars, as M. Liwschitz-Garik, Maltz-Herzog, Hellmund and E. M. Tingley [14–19], also contributed to the significant development of this area. Other interesting manual and/or automated methods and algorithms were developed later [20–24]. Each of these methods can be used for specific design constraints and none can be considered as universally valid. This is mainly due to the fact that, during the first seven decades of the 20th century, researchers were focused only on DC machines and single-phase, 2-phase and 3-phase AC machines. Nowadays, the interest is also directed towards multiphase machines, particularly with 5, 6 and 7-phases [21,22,25–27].

The cited winding design methods provide relevant drawbacks and difficulties if they are applied for these new winding configurations. In this context, we propose a simple, powerful and general procedure suitable for all symmetrical winding configurations, covering also concentrated topologies and even reduced or normal (radial symmetrical) systems [22,28]. Indeed, a hint of a similar method was fleetingly introduced by F. Heiles in [29]; however, he never developed it and later researchers, unexpectedly, did not give it an adequate consideration. The proposed method, namely WDT (Winding Distribution Table), allows the design of all m -phase single or double-layer windings, providing fast and automated winding designs. Moreover, by manipulating the WDT with simple procedures, it is possible to implement optimization techniques, such as: chording (coil pitch shortening), zone widening (coil side shift in a slot), interspersing¹ (or imbrication) [3,6,9,20,30,31] and double chording [16] (consisting on the adoption of both chording and interspersing [9,20]). The procedure for the determination of the WDT and its use are hereafter presented and, in order to validate this procedure, the comparison with the traditional star of slots method is provided with several examples, highlighting the fact that the latter is much more complex to construct because of several geometrical issues. More in detail, this paper is structured as follows: the general conditions allowing the definition of the winding configuration are described in Section 2, the proposed WDT procedure is described in detail in Section 3 and the validation of the procedure through the description of several examples of symmetrical windings is provided in Section 4.

2. Symmetry Conditions for Winding Design

For an electrical machine with N slots, m phases, i layers and p pole pairs, the winding symmetry can be evaluated by using the factors γ , namely the number of wound coils per phase, and g , which are defined, respectively, as:

$$\gamma = i \frac{N - \eta}{2m} \quad (1)$$

$$g = \begin{cases} \frac{iN}{2mt} & \text{for normal and non-reduced systems}^2 \\ \frac{N}{2mt} & \text{for reduced systems,} \end{cases} \quad (2)$$

where η represents the number of empty slots (dead-coil winding) in the case of single layer windings, and the number of unwound coils, in case of double layer windings and:

$$t = \gcd(N, p), \quad (3)$$

is the greatest common divider between N and p , whereas $i = 1, 2$ is the number of layers.

The winding symmetry is assessed with the help of the following conditions:

¹ i.e. transfer of one or more coils to another zone [28].

² as defined in [27,28]

$$\begin{cases} \gamma \in \mathbb{N} & \text{for coil windings} \\ \gamma \in \{\mathbb{N}, \mathbb{N}/2\} & \text{for bar windings,} \end{cases} \quad (4)$$

and

$$\begin{cases} g \in \mathbb{N} & \text{for symmetrical windings} \\ g \notin \mathbb{N} & \text{for unsymmetrical windings,} \end{cases} \quad (5)$$

where \mathbb{N} is the set of natural numbers.

If conditions (4) and the first of Eq. (5) are satisfied, the winding is symmetrical; otherwise, it is asymmetrical. In any case, for the computation of (1), the initial value of the empty slots η is assigned equal to zero. If (4) is not satisfied, then the value of η must be determined through formula

$$\eta = N - \frac{2 \cdot m \cdot \lfloor \gamma \rfloor}{i}, \quad (6)$$

where $\lfloor \gamma \rfloor$ is the largest integer less than or equal to γ . In this way, considering empty slots or unwound coils, the first condition of winding symmetry expressed by (4) is always satisfied. It must be underlined that (6) is valid only if $m > 1$.

The assignment of η between the different phases can be arbitrary if $\eta \neq m$ (even if the distribution of the empty slots should be as uniform as possible among the phase sections). If $\eta = m$, the empty slots should be chosen one for each phase (uniformly distributed), so that the corresponding slot EMF phasors are phase-shifted by $2\pi/m = 360^\circ/m$ in case of normal systems and by $\pi/m = 180^\circ/m$ in case of reduced systems.

An exception is valid if $m = 1$ (single phase windings), for which the following equation has to be considered in place of (6):

$$\eta = \left\lfloor \frac{N}{3} \right\rfloor, \quad (7)$$

where a winding covering $2/3$ of the slots is considered.

The number of wound slots per pole per phase is determined as

$$q = \frac{N - \eta}{2p \cdot m} = \frac{\gamma}{i \cdot p} = a + \frac{z}{i \cdot p}, \quad (8)$$

where $a = \lfloor q \rfloor$ and $z/i \cdot p$ is a proper fraction. If q is an integer number, then the winding is called “integral slot winding”. Otherwise, if q is a fractional number, the winding is defined as “fractional slot winding”.

Moreover, in the cases where $\eta > 0$, it is advantageous to define the number of slots per pole per phase given by

$$Q = \frac{N}{2p \cdot m} = \frac{\gamma}{i \cdot p} + \frac{\eta}{2p \cdot m} = q + \frac{\eta}{2p \cdot m}. \quad (9)$$

If $\eta = 0$, then $Q = q$.

In order to recognize basic winding configurations when q is a fractional number and $\eta = 0$, the following equation must be taken into account (considering (8)):

$$z = i \cdot p \cdot (q - a) = \gamma - i \cdot p \cdot a, \quad (10)$$

which gives the numerator of the proper fraction contained in (8). In this equation the case $i = 2$ can be referred both to double-layer windings and to single-layer bar windings when $\gamma \in \mathbb{N}/2$. In the last case, with $\eta = 0$, $i = 1$ and $k \in \mathbb{N}$, relation (1) becomes

$$\gamma = \frac{k}{2} = \frac{N}{2m},$$

or

$$\frac{N}{m} = k \in \mathbb{N},$$

which meets condition (1) for double layer windings. Furthermore, the factor t' must be defined for fractional slot windings:

$$t' = \gcd(z, p). \quad (11)$$

If $t' = 1$, the winding is a basic one. Otherwise, the winding is composed by t' repetitions of the same basic winding, which is composed by $N' = N/t'$ slots and $p' = p/t'$ pole pairs. If $\eta > 0$ then it is sometimes convenient to set $t' = 1$ in order to avoid the case $\eta > m$ (a case in which there would be too much unwound slots or coils).

For integer slot windings ($q \in \mathbb{N}$ and $\eta = 0$) the number of repetitions is equal to $t' = p$, because N and p have the same divisor equal to p itself as can be deduced by (8).

3. WDT Procedure

The proposed winding distribution procedure is based on the construction of a Winding Distribution Table (WDT), which allows the assignment of a specific stator slot to a winding phase section [6,23]. Hereafter the basic rules to determine the WDT are defined.

3.1. Determination of WDT

This table, containing N elements, is composed by a number of rows equal to m and a number of columns equal to

$$n_c = \frac{N}{m}, \quad (12)$$

whose elements are ordered as shown in Table 1.

Table 1. Order of the WDT elements.

	col. 1	col. 2	...	col. n_c
row 1	1	2	...	n_c
row 2	$n_c + 1$	$n_c + 2$...	$2n_c$
row 3	$2n_c + 1$	$2n_c + 2$...	$3n_c$
\vdots	\vdots	\vdots	\ddots	\vdots
row m	$(m-1)n_c + 1$	$(m-1)n_c + 2$...	mn_c

In the case of a single-layer winding, the WDT elements are referred to phasors associated to each slot or, in other words, to each coil side: a single-layer machine winding is composed by $N = 2m \cdot \gamma$ coils. In the double-layer winding configuration, the WDT elements are referred to a coil side, whereas the second coil side is defined by the coil pitch y_c usually expressed in terms of number of slots. In this case, the machine winding is composed by $N = m \cdot \gamma$ coils.

The definition of the WDT starts by assigning the slot number 1 to the first cell of Table 1. Then, the slot number 2 is assigned to the cell whose distance is equal to p cells from the first one, the slot number 3 to the cell whose distance is equal to p cells from the second one, following the orientation of the progressive numbering of the cells of Table 1. After N/p (if $N/p \in \mathbb{N}$) assignments, the procedure continues by imagining that the last cell of the table is ideally consecutive to the first: therefore, once the N -th table element is counted, the counting continues restarting from the first cell of the table. If the count ends in a filled cell, the adjacent empty cell will be filled with the counted slot. The procedure continues until the table is completely filled by the slot numbers.

126 In order to clarify this procedure, Table 2 reports the WDT referred to a simple integral slot
127 symmetrical winding with $N = 24$, $p = 2$, $m = 3$ and $q = 2$. The Table is filled in $p = 2$ filling
128 cycles, each one corresponding to $N/p = 12$ assignments. In fact, by starting from placing slot nr. 1
129 in the first cell (row 1, col. 1), the slot nr. 2 is placed after $p = 2$ cells (row 1, col. 3), till slot nr. 12
130 is assigned to the 23-th cell (row 3, col. 7), which corresponds to the N/p -th assignment and the first
131 filling cycle is completed. The second cycle starts by counting p elements from cell nr. 23, which
132 corresponds to element nr. 25. However, due to the periodicity of this winding configuration ($N = 24$),
133 the element nr. 25 corresponds to the first element. Therefore, the slot nr. 13 will be placed in the
134 adjacent empty second cell (row 1, col. 2). The vertical double bar separates the active conductors
135 with positive EMF from those with negative EMF. In symmetrical windings, the double bar should be
136 located around the middle of the table in order to gain the highest EMF. The star of slots corresponding
137 to this configuration is plotted in Figure 1. The positive EMFs are reported in a thicker width with
138 respect to the negative ones. It can be noticed, by comparing the rows of Table 2 with Figure 1, that the
139 WDT is the tabular and linear representation of the star of slots, therefore there is virtually no need to
140 use the star of slots. Anyway, hereinafter the stars of slots will be represented only for more clarity.

Table 2. Winding Distribution Table for a winding with $N = 24$, $p = 2$ and $m = 3$.

1	13	2	14	3	15	4	16
5	17	6	18	7	19	8	20
9	21	10	22	11	23	12	24

(phase 1: blue, phase 2: green, phase 3: red)

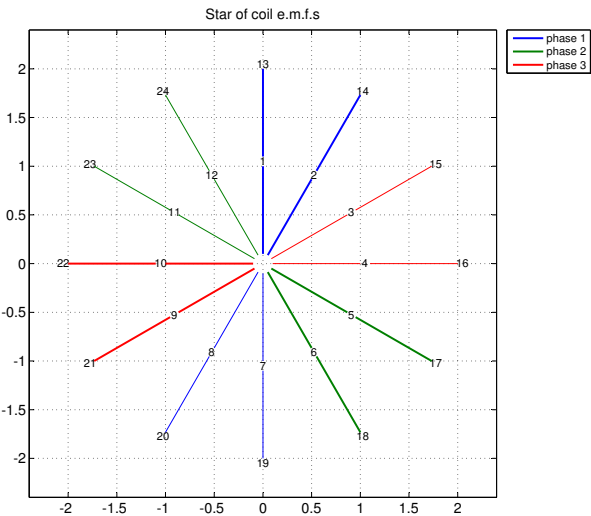


Figure 1. Plot of the EMF star for a symmetrical winding with $N = 24$, $m = 3$ and $p = 2$.

141 The parameter t given in (3) determines the number of superposing EMF stars related to the
142 specific winding configuration. Therefore, in the WDT, the slots associated to the cells from $kt + 1$
143 to $(k + 1)t$ (with $k = 0, 1, 2, \dots, N/t - 1$) will have the same phase-angle, by following the WDT path
144 previously defined and shown in Table 2. In particular, each EMF star is composed by N/t phasors,
145 phase-shifted to each other by an electrical angle α equal to

$$\alpha = t \cdot \frac{360^\circ}{N}. \tag{13}$$

146 By following these considerations it is possible to reconfigure Table 1 and to build Table 3 as
147 used in [3,6], in which the electrical angles φ_k of each slot-phasor pair are computed by the following
148 formula:

$$\varphi_k = k \cdot \alpha \text{ with } k = 0, 1, \dots, N/t - 1. \quad (14)$$

149

Table 3. Electrical angles of the star of slots ($j = 1, \dots, t$).

φ_k	0°	α	2α	\dots	$(N/t - 1)\alpha$
1-st row	1	2	3	\dots	N/t
\vdots	\vdots	\vdots	\vdots	\ddots	\vdots
t -th row	$(j-1)N/t + 1$	$(j-1)N/t + 2$	$(j-1)N/t + 3$	\dots	N

150 With reference to the previous example, it can be noticed that each EMF star is composed by
 151 $N/t = 24/2 = 12$ phasors, phase-shifted to each other by an electrical angle α equal to

$$\alpha = t \cdot \frac{360^\circ}{N} = 30^\circ. \quad (15)$$

152 Therefore, $t = 2$ represents the number of phasors having equal phases. In this example (see Table
 153 2), the pair of phasors 1-13, 2-14, 3-15, 4-16... have the same phase-shift. Moreover, the consecutive
 154 pairs are shifted between each other by an angle equal to 30° , as shown in Fig. 1 (i.e., the pair 2-14 is
 155 phase-shifted by an angle of 30° with the pair 1-13). Thus, the phase-shifts of all phasors can be easily
 156 computed by considering Table 3. The resulting table is shown in Table 4.

Table 4. Electrical angles of the EMF star phasors for $N = 24$, $p = 2$ and $m = 3$.

Electr. angles φ_k	0°	30°	60°	90°	120°	150°	180°	210°	240°	270°	300°	330°
Phasor pairs	1 13	2 14	3 15	4 16	5 17	6 18	7 19	8 20	9 21	10 22	11 23	12 24

157 In truth, by considering that $q = 2$, the same WDT can be obtained considering the number of
 158 repetitions t' as defined by formula (11). In fact, this winding can be seen as composed by $t' = 2$
 159 repetitions of the same winding characterized by $N' = N/t' = 24/2 = 12$ slots, $m = 3$ phases and
 160 $p' = p/t' = 2/2 = 1$ pole pair ($\gamma' = \gamma/t' = 4$) and, therefore, the WDT can be seen as the composition
 161 of two basic WDTs as shown in Table 5. In this case the second WDT is created with the same rules
 162 above exposed but starting from slot $N/2 + 1$ till slot N . Now, by considering the two repetitions, this
 163 winding could be divided in two parallel connected branches. A comparison of Tables 2 and 5 shows
 164 their equivalence.

Table 5. Winding Distribution Table with $t' = 2$ repetitions, for a winding with $N = 24$, $p = 2$ and $m = 3$.

1	2	3	4	13	14	15	16
5	6	7	8	17	18	19	20
9	10	11	12	21	22	23	24

(phase 1: blue, phase 2: green, phase 3: red)

165 It will be demonstrated in the following sections that simple computations allow the determination
 166 of the winding distribution even for complex configurations.

167 3.2. WDT Post-processing

168 After the WDT is created, the winding factors of the $\nu - th$ harmonic and the related proper
 169 phases for each $h - th$ phase can be computed through the following equations:

$$k_{wpv,h} = \frac{1}{2pqi} \cdot \sqrt{\left(\sum_{n=1}^{2pqi} C_{pv,h,n}\right)^2 + \left(\sum_{n=1}^{2pqi} S_{pv,h,n}\right)^2} \quad (16)$$

and

$$\arg(k_{wpv,h}) = \text{atan2}\left(\sum_{n=1}^{2pqi} S_{pv,h,n}, \sum_{n=1}^{2pqi} C_{pv,h,n}\right), \quad (17)$$

where:

$$C_{pv,h,n} = k \cdot \cos\left(2\pi pv \frac{|a_{h,n}|}{N}\right), \quad (18)$$

$$S_{pv,h,n} = k \cdot \sin\left(2\pi pv \frac{|a_{h,n}|}{N}\right), \quad (19)$$

$$k = \begin{cases} +1 & \text{if } a_{h,n} > 0 \\ -1 & \text{if } a_{h,n} < 0, \end{cases} \quad (20)$$

$a_{h,n}$ is a generic element of the WDT, $n = 1, 2, \dots, N/m$ is the n -th column of the WDT and $h = 1 \dots m$ is the h -th phase of the related winding. If the winding is symmetrical, the computation of harmonic winding factors can be limited to only one phase (for example the 1-st phase, i.e. $h = 1$). When dealing with double layer windings, also the negative coil sides (defined by their coil pitch y_c) have to be inserted in the WDT.

3.3. WDT for Symmetrical Non-reduced and Normal Systems

In the case of radially symmetrical or normal systems, in order to visualize, if required, all the positive and the negative phasors of the same phase in the same row, an adequate number of the last WDT columns (these group of columns are indicated in Figure 2 as “right side”) must all be shifted in the upper direction by ζ shifts (see Figure 2) and their sign must be changed, where

$$\zeta = \begin{cases} \frac{m-1}{2} & \text{if } m \in \mathbb{U} \\ \frac{m}{2} - 1 & \text{if } m \in \mathbb{G}. \end{cases} \quad (21)$$

The number of columns to be shifted depends on the type of winding. In the case of a single layer symmetrical winding, $N/2m = \gamma$ columns must be shifted, due to the fact that the number of positive slots must be equal to the negative ones and the WDT will be divided into two equal left and right sides. In the case of a single layer bar winding, it may happens that γ be a fraction with the denominator equal to 2. Therefore, $\gamma \pm 1 = N/2m \pm 1$ columns should be shifted. For the double-layer configuration, this restriction is not necessary. Therefore, the number of positive and negative coils can be chosen properly, depending on the type of winding design optimization (maximization of the EMF, reduction of the harmonic content, simplicity of realization of end windings, zone widening, etc.). In addition, in any case, a minus sign is added to the shifted columns, so that the coil sides with the negative EMF can be explicitly visualized within the WDT. It clearly appears that the groups of adjacent elements with the same sign located in each row of the WDT represent the winding zones of each phase. It should be noted that, in case of bar or double-layer windings, the number of columns of the “left” and “right” side are, in general, given by $\lfloor N/m \rfloor$ and $\lceil N/m \rceil$, respectively, or *vice versa* (see Figure 2).

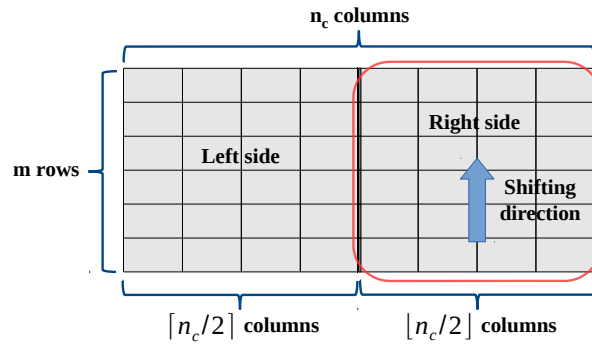


Figure 2. WDT for a generic normal system winding. The right side of WDT is shifted upwards by ζ steps.

3.4. WDT for Reduced Systems

For reduced systems the WDT is not affected by vertical shifting, but the quadrants named 1 and 3 in Figure 3 are simply swapped. In this case the WDT is valid for all windings with $m \in \mathbb{G}$ (for example in two-, four- or six-phase reduced system windings). The sign of the slot numbers in Quadrants 1 and 4 are then changed to account for negative coil sides. It should be noted that, in case of bar or double-layer windings, the number of columns of Quadrants 1 and 4 is, in general, given by $\lceil N/m \rceil$, whereas the number of columns of Quadrants 2 and 3 by $\lfloor N/m \rfloor$ or *vice versa*. After this operation the rows of the WDT should be reordered following the procedure of Table 6.

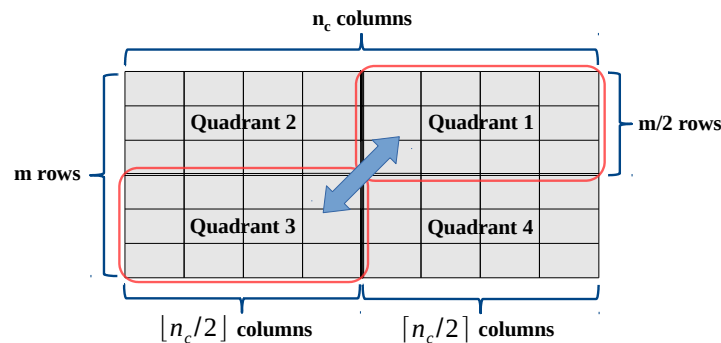


Figure 3. Swapping of the WDT quadrants in case of reduced systems and $m \in \mathbb{G}$.

Reduced system whose number of phases is not a power of 2 are composed by m_g groups of m_u -phase systems shifted by an angle of

$$\alpha_g = \frac{\pi}{m} = \frac{180^\circ}{m}, \quad (22)$$

where

$$m_u = \text{gpf}(m), \quad (23)$$

is the greatest prime factor of m , and

$$m_g = \frac{m}{m_u}. \quad (24)$$

For example a reduced system winding with $m = 10$ phases can be decomposed into $m_g = 2$ groups of $m_u = 5$ -phase systems; a reduced system winding with $m = 12$ phases can be decomposed into $m_g = 4$ groups of $m_u = 3$ -phase systems. The even groups of a reduced system must then be

Table 6. Reordering of the rows of a WDT for an m -phase reduced system winging with $m \in \mathbb{G}$.

Phases	col. 1	col. 1	...	col. n_c		Phases	col. 1	col. 1	...	col. n_c
1		1
\vdots	\vdots	\vdots	\ddots	...		$\frac{m}{2} + 1$
$\frac{m}{2}$	\Rightarrow	2
$\frac{m}{2} + 1$		$\frac{m}{2} + 2$
\vdots	\vdots	\vdots	\ddots	...		\vdots	\vdots	\vdots	\ddots	...
m		$\frac{m}{2}$
						m

multiplied by -1 in order to make them radially symmetrical. The procedure will be cleared in Section 4.

3.5. WDT for Single-phase Systems

For $m = 1$, the WDT is reduced to a single row composed by four sectors, as shown in Figure 4: the first sector is composed by $\lceil (N-\eta)/2 \rceil$ cells, the second by $\lfloor \eta/2 \rfloor$ (or $\lceil \eta/2 \rceil$) cells (representing empty slots of the first unwound part), the third by $\lfloor (N-\eta)/2 \rfloor$ cells and the last one by $\lceil \eta/2 \rceil$ (or $\lfloor \eta/2 \rfloor$) cells (representing empty slots of the second unwound part).

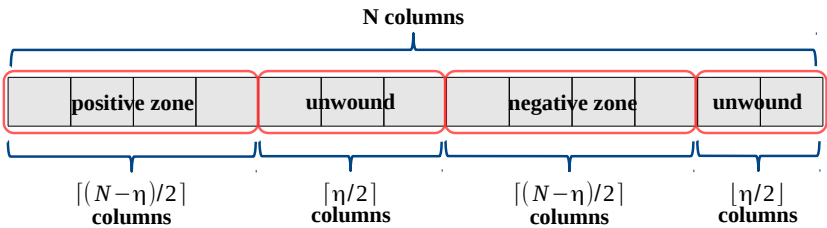


Figure 4. A possible WDT for single phase windings.

Another simple possible procedure to solve single phase windings is to consider them as derived from a three-phase winding, but excluding one phase (therefore, the “starting phase” can be located in the unwound slots). An example of this approach will be shown and discussed in the last example of Section 4.

4. Examples and Procedure Validation

In this Section several examples of winding configurations for electrical machines are reported in order to validate the proposed procedure. These examples can be adequate for the comprehension of the modality of construction of the WDT for each of the proposed electrical machine. Other more complex examples for multiphase windings are also considered and analyzed in the following subsections. The construction of the EMF stars and the representation in plane of the related winding configuration are used as references for the procedure validation.

4.1. 3-phase Windings

An electrical machine composed by 24 stator slots and 2 pole pairs, equipped with a three-phase winding with $q = 2$, is used as a first validation test, which is symmetrical because $\gamma \in \mathbb{N}$ and $g \in \mathbb{N}$. The corresponding WDT has been already determined in Subsection 3.1. The data needed for the WDT construction and its related properties can be summarized as follows: $N = 24$, $m = 3$, $p = 2$, $\gamma = 8$, $t = 2$, $\alpha = 30^\circ$, $\alpha' = 30^\circ$, $\zeta = 1$. Therefore, the corresponding WDT is composed by $m = 3$ rows and $N/m = 8$ columns, with a cell pitch equal to $p = 2$, as shown in Table 2. This winding is composed by $\gamma = 8$ coils per phase, which means $m \cdot \gamma = 3 \cdot 8 = 24$ overall coils. The EMF of each coil is represented by a phasor in the star of slots, as shown in Figure 1, which is, therefore, composed by 8 EMF phasors

for each phase and by the superposition of two stars of coil EMFs ($t = 2$), where each one contains twelve phasors equally phase-shifted between each others by 30° ($\alpha' = 30^\circ$). The EMFs corresponding to the slots 1, 2, 3, ..., 12 will have the same phase angle of the EMFs located in the slots 13, 14, 15, ..., 24, respectively. Therefore, the elements of the Table can be regrouped in 12 groups composed by $t = 2$ elements and by following the order of the Table, the linear representation of the star of slots can be detected, as it can be seen by comparing Table 2 with Figure 1.

In Table 2, the phasors (or slots) of phase 1 are written in blue color, while the phasors of phase 2 and 3 are reported in green and red colors, respectively. In order to visualize the phasors of the same phase in a single WDT row, the last 4 columns ($N/2m = 4$) of the WDT should be circularly shifted in the upper direction by a quantity equal to $\zeta = 1$ as calculated by applying (21) and that can be deduced by analyzing Table 2. The winding scheme is visualized in Figure 5a.

As previously mentioned, the WDT can be referred to both single-layer and double-layer windings. Indeed, for double layer configuration, the position of the left side of a coil is defined by the number corresponding to the slot, whereas the position of right side is defined by the coil pitch y_c , which is equal, in most cases, to $5/6 \cdot y_p$ (a shortened pitch employed for the limitation of both the 5-th and 7-th harmonics), where $y_p = N/2p$ is the pole pitch expressed in terms of number of slots. An example of double-layer winding scheme is plotted in Figure 5b, where $y_c = 5$.

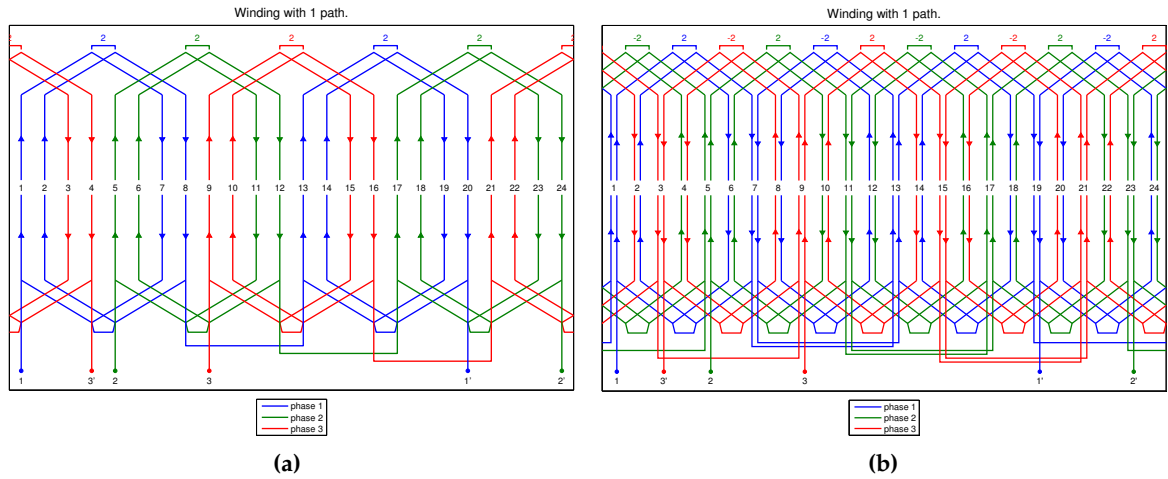


Figure 5. Winding scheme with $N = 24$, $m = 3$, $p = 2$ and $q = 2$ for: (a) single-layer configuration, (b) double-layer configuration with $y_c = 5$.

Tables 7 and 8 show the WDT referred to a three-phase winding with $N = 27$, $p = 3$, for a single-layer and a double-layer configuration, respectively. It can be noticed that, in case of single-layer coil winding, three empty slots are required ($\eta = 3$) in order to satisfy the symmetry conditions. The corresponding unwound slots are highlighted by the crossed elements of Table 7. The winding is therefore composed by the same number of positive and negative slots. Here $Q = 1 + 1/2$ and $q = 2$. The corresponding star of slots achieved from the two WDT Table and the related winding scheme are plotted in Figures 6a and 6b.

Table 7. WDT for a single-layer, three-phase winding with $N = 27$, $m = 3$ and $p = 3$.

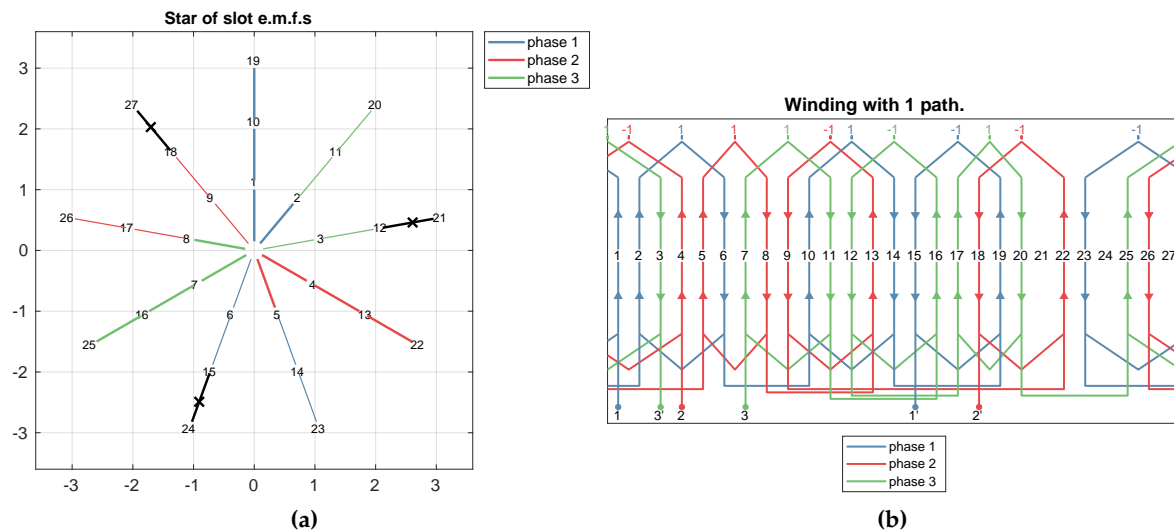
1	10	19	2	-11	-20	-3	-12	24
4	13	22	5	-14	-23	-6	-15	24
7	16	25	8	-17	-26	-9	-18	24

(ph1: blue, ph2: red, ph3: green) $\uparrow \zeta = 1$

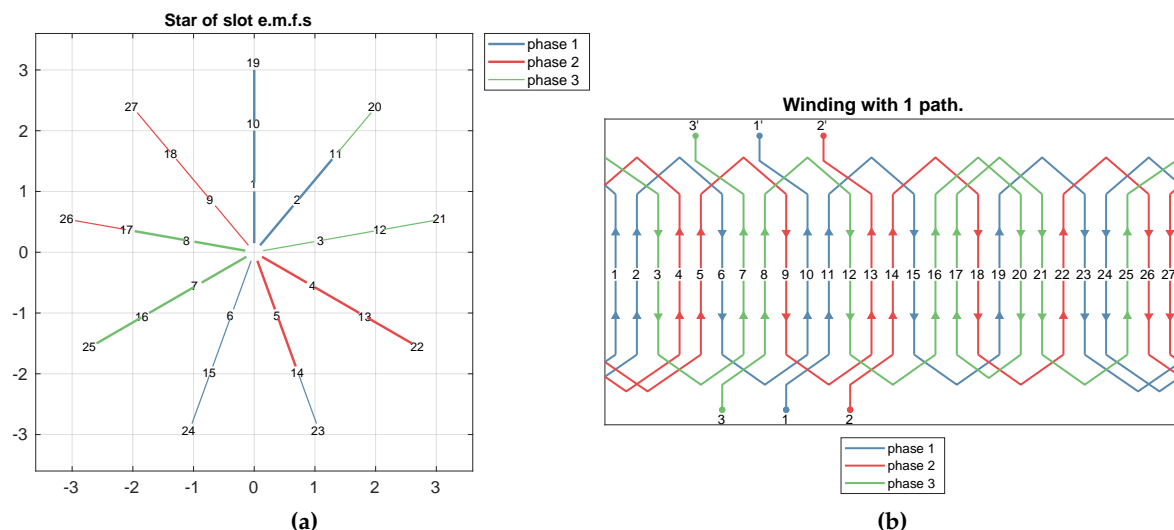
Table 8. WDT for a double-layer, three-phase winding with $N = 27$, $m = 3$ and $p = 3$

$$\begin{array}{c|c|c} 1 & 2 & -3 \\ \hline 4 & 5 & -6 \\ \hline 7 & 8 & -9 \end{array} + \begin{array}{c|c|c} 10 & 11 & -12 \\ \hline 13 & 14 & -15 \\ \hline 16 & 17 & -18 \end{array} + \begin{array}{c|c|c} 19 & 20 & -21 \\ \hline 22 & 23 & -24 \\ \hline 25 & 26 & -27 \end{array} = \begin{array}{c|c|c|c|c|c|c|c|c} 1 & 10 & 19 & 2 & 11 & 20 & -3 & -12 & 21 \\ \hline 4 & 13 & 22 & 5 & 14 & 23 & -6 & -15 & 24 \\ \hline 7 & 16 & 25 & 8 & 17 & 26 & -9 & -18 & -27 \end{array} \uparrow \zeta = 1$$

(ph1: blue, ph2: red, ph3: green)

**Figure 6.** (a) Slot EMF star for a symmetrical single-layer coil winding and (b) winding scheme. $N = 27$, $m = 3$, $p = 3$, $Q = 1 + 1/2$ and $q = 2$.

If it is necessary to fill also the empty slots only a bar winding can be here considered as shown in Figures 7a and 7b. In fact, only in case of single layer bar windings, γ can be a fractional number with denominator equal to 2.

**Figure 7.** (a) Slot EMF star for a symmetrical single-layer bar winding and (b) winding scheme. $N = 27$, $m = 3$, $p = 3$ and $q = 1 + 1/2$.

Figures 8a and 8b refer to the double layer configuration with a coil pitch $y_c = 4$, which is composed by 3 repetitions of the basic winding with $N' = N/\iota' = 27/3 = 9$ slots, $m = 3$ phases and $p' = p/\iota' = 3/3 = 1$ pole pair. The WDT is composed by the repetition of 3 basic WDTs: the first is

266 created considering the slot range $1 \dots N/t'$, the second by the slot range $N/t' + 1 \dots 2N/t'$ and the third
267 $2N/t' + 1 \dots 3N/t'$. More generally, the t' slot ranges are given by $(k - 1)N/t' + 1 \dots kN/t'$ with $k = 1, \dots, t'$.
268 If necessary, this winding could be divided in three parallel connected paths: then, each path will be
269 identified by the three WDTs shown in Table 8. Figure 8b refers to a series connection of the three
270 paths.

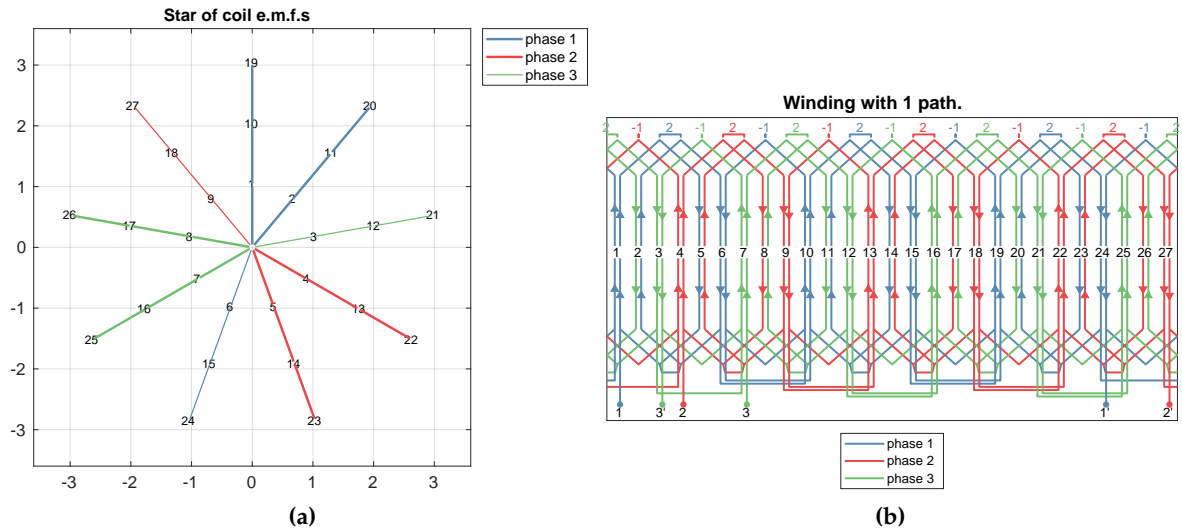


Figure 8. (a) Coil EMF star for a symmetrical double-layer coil winding and (b) winding scheme with series connected paths. $N = 27, m = 3, p = 3, q = 1 + 1/2$ and $y_c = 4$.

271 The WDT method is also suitable to design fractional single and double layer concentrated
272 windings. Figures 9a and 9b show, for example, a single layer concentrated winding with $N = 24$,
273 $m = 3, p = 11, \gamma = N/m = 24/3 = 8$ and $q = 4/11$. The related WDT is represented in Table 9.

Table 9. WDT for a single-layer, three-phase winding with $N = 24, m = 3$ and $p = 11$.

1	12	23	10	-21	-8	-19	-6
17	4	15	2	-13	-24	-11	-22
9	20	7	18	-5	-16	-3	-14

(ph1: blue, ph2: red, ph3: green) $\uparrow \zeta = 1$

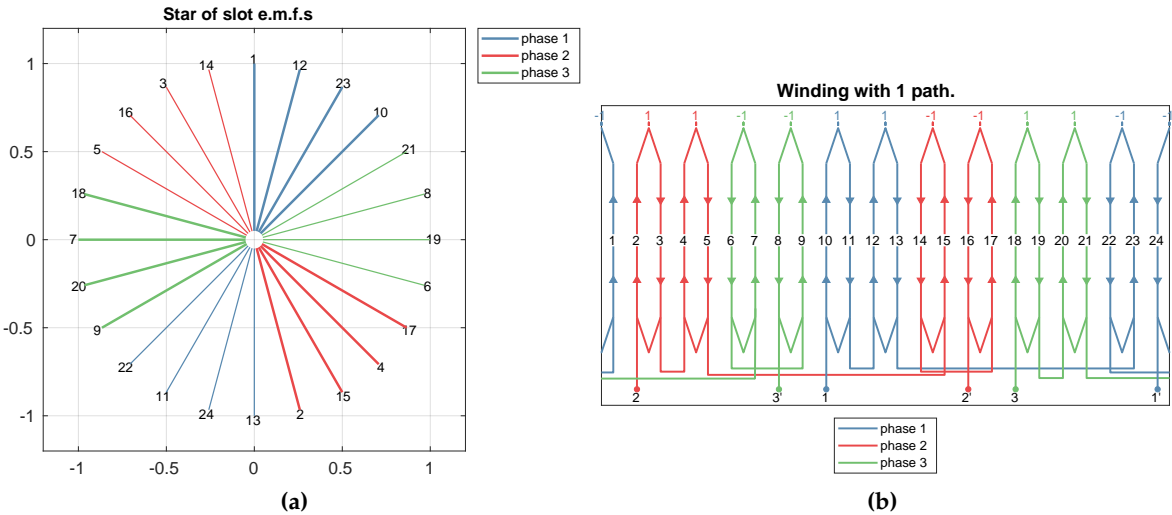


Figure 9. (a) Slot EMF star for a symmetrical single-layer concentrated coil winding and (b) winding scheme. $N = 24, m = 3, p = 11$ and $q = 4/11$.

4.2. 6-phase Windings

An example of WDT applied to multiphase winding configurations is reported in Table 10, which shows the WDT for a six-phase, non-reduced winding with $N = 36, p = 5, \gamma = 3$ and $q = 3/5$, whose corresponding star of slot is shown in Figure 10a.

By applying now the swapping procedure to Table 10 (without shifting) and the phases reordering following Table 6 described in Subsection 3.4, and by changing the sign of rows 3 and 4 in order to achieve a radial symmetry (as general rule the WDT rows of the even numbered phase groups are multiplied by -1), it is possible to determine the WDT referred to the reduced winding configuration, shown in Table 11. The star of slots referred to this type of winding is plotted in Figure 10b. It can be noticed that this reduced configuration is composed by two groups ($m_g = 2$) of three-phase winding sections ($m_u = 3$), phase-shifted between each other by an angle corresponding to 30° : the first one is composed by phases 1-5-3, whereas the second group by phases 2-6-4.

Table 10. Winding Distribution Table for a symmetrical non-reduced winding with $N = 36, m = 6, p = 5$ and $q = 3/5$.

1	30	23	-16	-9	-2
31	24	17	-10	-3	-32
25	18	11	-4	-33	-26
19	12	5	-34	-27	-20
13	6	35	-28	-21	-14
7	36	29	-22	-15	-8

$\uparrow \zeta = 2$

(ph1: blue, ph2: green, ph3: red, ph4: cyan, ph5: magenta, ph6: yellow)

Table 11. Winding Distribution Table for a symmetrical reduced winding with $N = 36, m = 6, p = 5$ and $q = 3/5$.

1	30	23	-19	-12	-5
31	24	17	-13	-6	-35
25	18	11	-7	-36	-29
16	9	2	-34	-27	-20
10	3	32	-28	-21	-14
4	33	26	-22	-15	-8

 $\Rightarrow -1 \cdot \left\{ \begin{array}{ccc|ccc} 1 & 30 & 23 & -19 & -12 & -5 \\ 16 & 9 & 2 & -34 & -27 & -20 \\ -31 & -24 & -17 & 13 & 6 & 35 \\ -10 & -3 & -32 & 28 & 21 & 14 \\ 25 & 18 & 11 & -7 & -36 & -29 \\ 4 & 33 & 26 & -22 & -15 & -8 \end{array} \right.$

(ph1: blue, ph2: green, ph3: red, ph4: cyan, ph5: magenta, ph6: yellow)

Tables 10 and 11 can be now used to determine the winding configuration: here a single layer configuration has been chosen for the non reduced system winding, whereas a double layer one with coil pitch $y_c = 3$ has been chosen for the reduced system. The winding diagrams are shown in Figure 11a and in Figure 11b, respectively. In the case of the double layer winding, Table 11 shows only one side of the coils, i.e. the positive one, whereas the position of the other (the negative coil sides) depends on the chosen value of the coil pitch y_c .

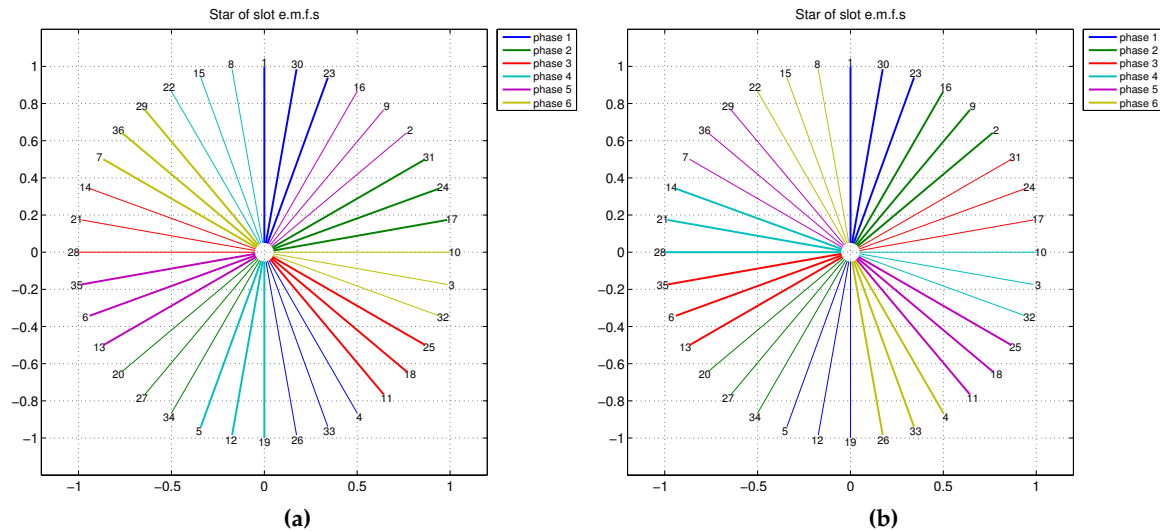


Figure 10. EMF stars for a symmetrical (a) non-reduced and (b) reduced winding with $N = 36$, $m = 6$, $p = 5$ and $q = 3/5$.

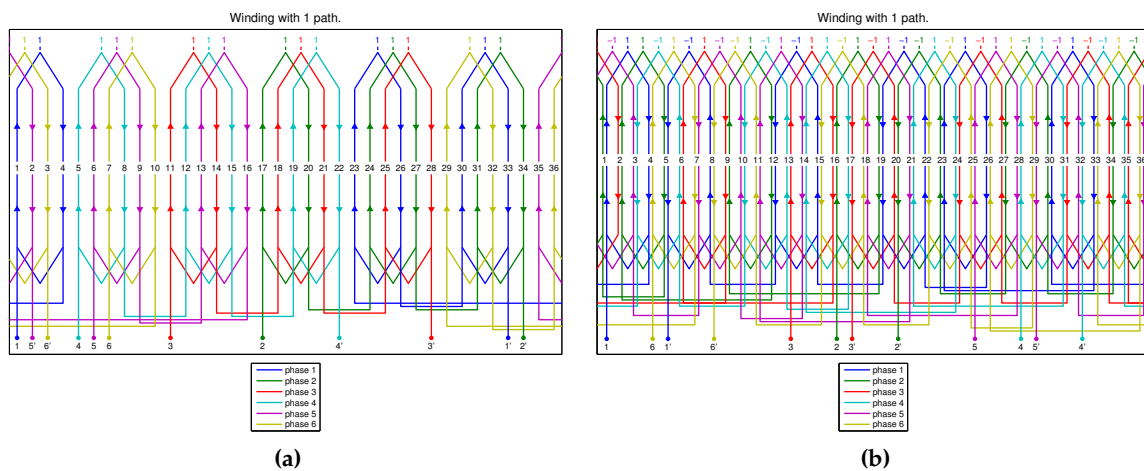


Figure 11. Winding schemes for (a) single layer non-reduced and (b) double layer reduced symmetrical configuration with $N = 36$, $m = 6$, $p = 5$ and $q = 3/5$.

4.3. 2-phase Winding

A reduced 2-phase double-layer winding is here considered, with $N = 28$, $p = 1$, $y_c = 12$. The WDT is represented in Table 12.

After swapping Quadrant 1 and 3 and changing the signs of Quadrants 1 and 4 the WDT becomes as shown in Table 13. Figure 12a represents the related star of slots and Figure 12b shows the double-layer winding scheme.

Table 12. WDT for a single-layer, 2-phase winding with $N = 28$ and $p = 1$, before swapping.

1	2	3	4	5	6	7	8	9	10	11	12	13	14
15	16	17	18	19	20	21	22	23	24	25	26	27	28

(ph1: blue, ph2: green)

Table 13. WDT for a single-layer, 2-phase winding with $N = 28$ and $p = 1$, after swapping.

1	2	3	4	5	6	7	-15	-16	-17	-18	-19	-20	-21
8	9	10	11	12	13	14	-22	-23	-24	-25	-26	-27	-28

(ph1: blue, ph2: green)

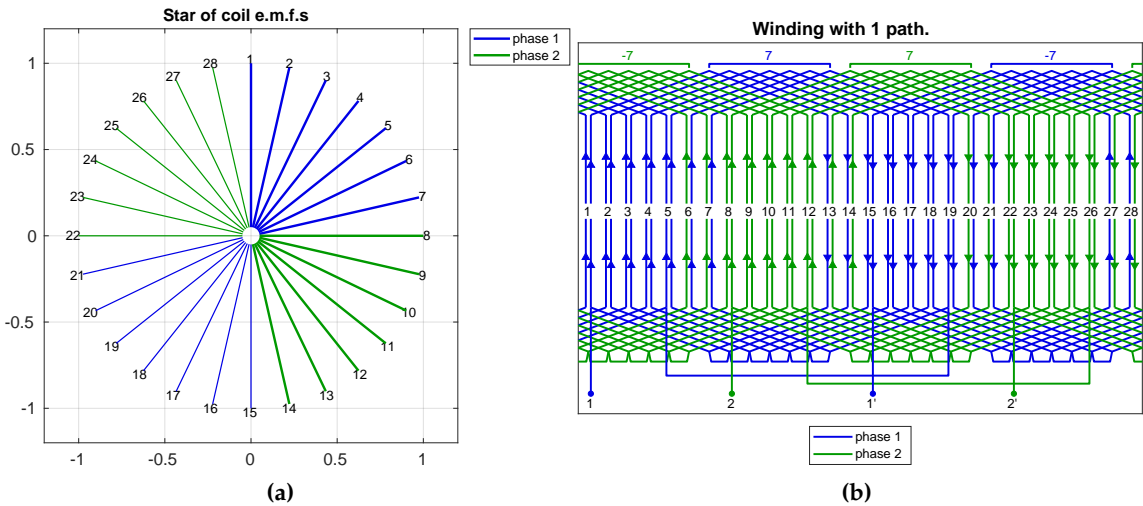


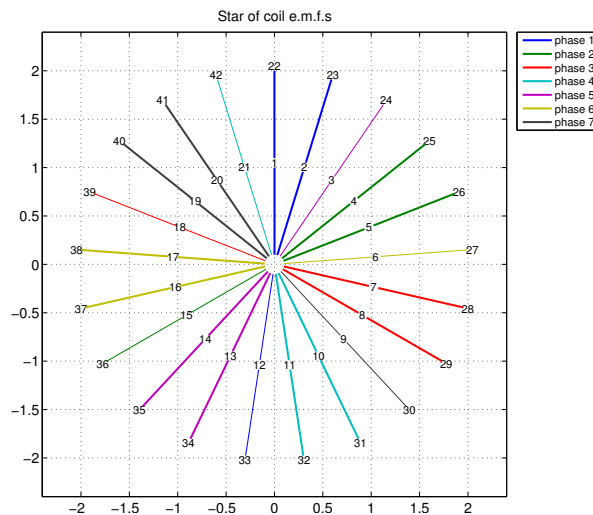
Figure 12. (a) Star of coils EMF and (b) Winding scheme for $N = 28$, $m = 2$, $p = 1$, $q = 7$ and $y_c = 12$.

Table 14. Winding Distribution Table for a double layer winding with $N = 42$, $p = 2$ and $m = 7$

1	2	3		22	23	24		1	22	2	23		3	24
4	5	6		25	26	27		4	25	5	26		6	27
7	8	9		28	29	30		7	28	8	29		9	30
10	11	12	+	31	32	33	=	10	31	11	32		12	33
13	14	15		34	35	36		13	34	14	35		15	36
16	17	18		37	38	39		16	37	17	38		18	39
19	20	21		40	41	42		19	40	20	41		21	42

$\uparrow \zeta = 3$

(ph1: blue, ph2: green, ph3: red, ph4: cyan, ph5: magenta, ph6: yellow, ph7: black)

**Figure 13.** Plot of the EMF star for a double layer seven-phase symmetrical winding with $N = 42$, $p = 2$, $m = 7$, $y_c = 9$ and $q = 1 + 1/2$.

4.4. 7-phase Winding

Another example consists in a seven-phase machine with 42 slots and 2 pole pairs. The WDT parameters can be easily determined by taking into account the equations described in Section 2. Therefore, the data needed for the WDT procedure are: $N = 42$; $m = 7$; $p = 2$; $\gamma = 6$; $t = 2$; $\alpha' = 17.14^\circ$; $t' = 2$; $\zeta = 3$.

Table 14 reports the WDT for this case of study. It is a 7x6 (rows x columns) table with a cell pitch equal to 2, with six coils composing a winding phase section and two stars of 21 EMF phasors, as shown in the diagram of Figure 13. By virtue of (11) the WDT can be divided into $t' = 2$ basic tables as shown in Table 15. The related double-layer winding scheme is depicted in Figure 14 with a chosen shortened coil pitch $y_c = 9$.

4.5. Procedures for Winding Optimization

The proposed procedure is also suitable for the implementation of winding optimization techniques, such as interspersing for single-layer windings and double chording for double layer windings. For instance, the WDT referred to a three-phase machine with $p = 5$ and a double-layer winding located into 72 slots is reported in Table 15, whereas the corresponding star of slots and winding scheme are plotted in Figures 15 and 16, respectively.

The double chording with $y_c = 6$ and a three-order single-sided imbrication is obtained by circularly shifting upwards by two cells and by changing the sign of the first $2 \cdot j$ elements of the left side of the WDT and the first j elements of the right side of the WDT (in this case, the elements of columns nr. 2, 4 and 6 for the left side and the elements of columns nr. 13, 14 and 15 of the right are

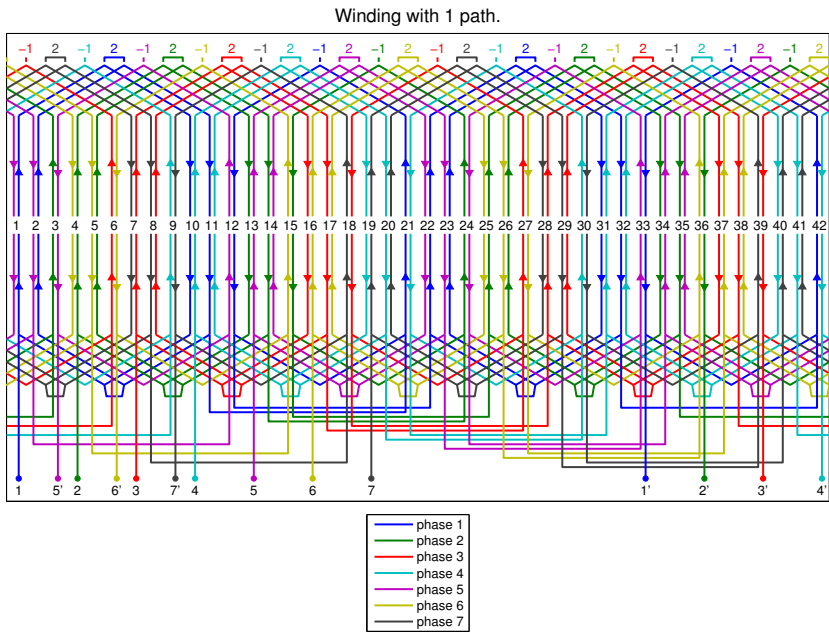


Figure 14. Winding scheme for a double-layer, seven-phase configuration with $N = 42$, $p = 2$, $m = 7$, $y_c = 9$ and $q = 1 + 1/2$.

Table 15. Winding Distribution Table for a winding with $N = 72$, $p = 5$ and $m = 3$

1	30	59	16	45	2	31	60	17	46	3	32	-37	-66	-23	-52	-9	-38	-67	-24	-53	-10	-39	-68
49	6	35	64	21	50	7	36	65	22	51	8	-13	-42	-71	-28	-57	-14	-43	-72	-29	-58	-15	-44
25	54	11	40	69	26	55	12	41	70	27	56	-61	-18	-47	-4	-33	-62	-19	-48	-5	-34	-63	-20

(ph1: blue, ph2: red, ph3: green)

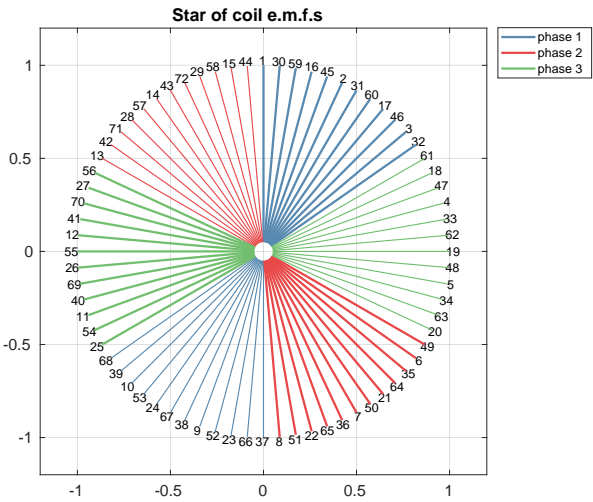


Figure 15. Plot of the EMF star for a three-phase symmetrical winding with $N = 72$, $p = 5$ and $m = 3$.

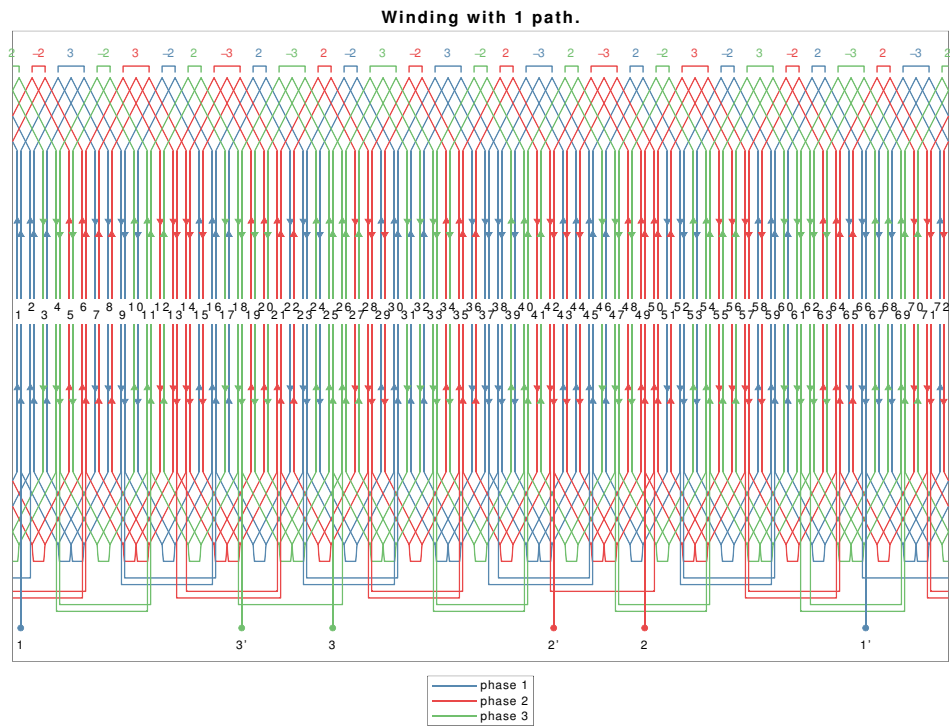


Figure 16. Winding scheme for a three-phase winding with $N = 72$, $p = 5$ and $m = 3$.

Table 16. Double chording with a 3-rd order single-sided imbrication for $N = 72$, $p = 5$ and $m = 3$

1	-54	59	-40	45	-26	31	60	17	46	3	32	61	18	47	-52	-9	-38	-67	-24	-53	-10	-39	-68
49	-30	35	-16	21	-2	7	36	65	22	51	8	37	66	23	-28	-57	-14	-43	-72	-29	-58	-15	-44
25	-6	11	-64	69	-50	55	12	41	71	27	56	13	42	71	-4	-33	-62	-19	-48	-5	-34	-63	-20
	↑		↑		↑							↑	↑	↑									

(ph1: blue, ph2: red, ph3: green)

both circularly shifted and changed in sign), according to Table 16. Indeed, the corresponding star of slots is plotted in Figure 17, whereas the modified winding scheme is plotted in Figure 18.

Moreover, by shifting the WDT elements in accordance to Table 17, it is possible to implement a double chording technique with $y_c = 6$ and a double-sided imbrication with order equal to 3. This case differs from the previous one (single-sided imbrication) by the fact that the $2 \cdot j$ columns are circularly shifted for each side of the WDT, as shown by the arrows of Table 17. The corresponding star of slots and winding scheme are depicted in Figures 19 and 20, respectively.

A triple chording can be performed in order to further reduce the winding harmonic content with the following procedures whose results are given in Table 18:

1. the WDT is developed;
2. the zone widening by two slots is performed by shifting the double bar from the middle position to the right by two cells;

Table 17. Double chording with a 3-rd order double-sided imbrication for $N = 72$, $p = 5$ and $m = 3$

1	-54	59	-40	45	-26	31	60	17	46	3	32	-37	18	-23	4	-9	62	-67	-24	-53	-10	-39	-68
49	-30	35	-16	21	-2	7	36	65	22	51	8	-13	66	-71	52	-57	38	-43	-72	-29	-58	-15	-44
25	-6	11	-64	69	-50	55	12	41	71	27	56	-61	42	-47	28	-33	14	-19	-48	-5	-34	-63	-20
	↑		↑		↑							↑		↑	↑		↑						

(ph1: blue, ph2: red, ph3: green)

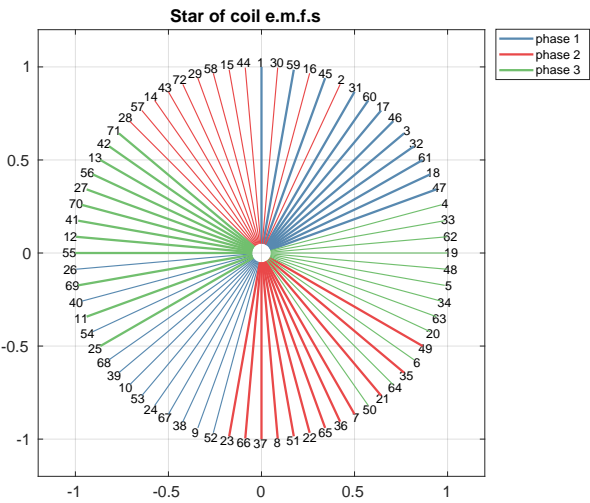


Figure 17. Double chording with a 3rd-order single-sided imbrication for $N = 72$, $p = 5$ and $m = 3$.

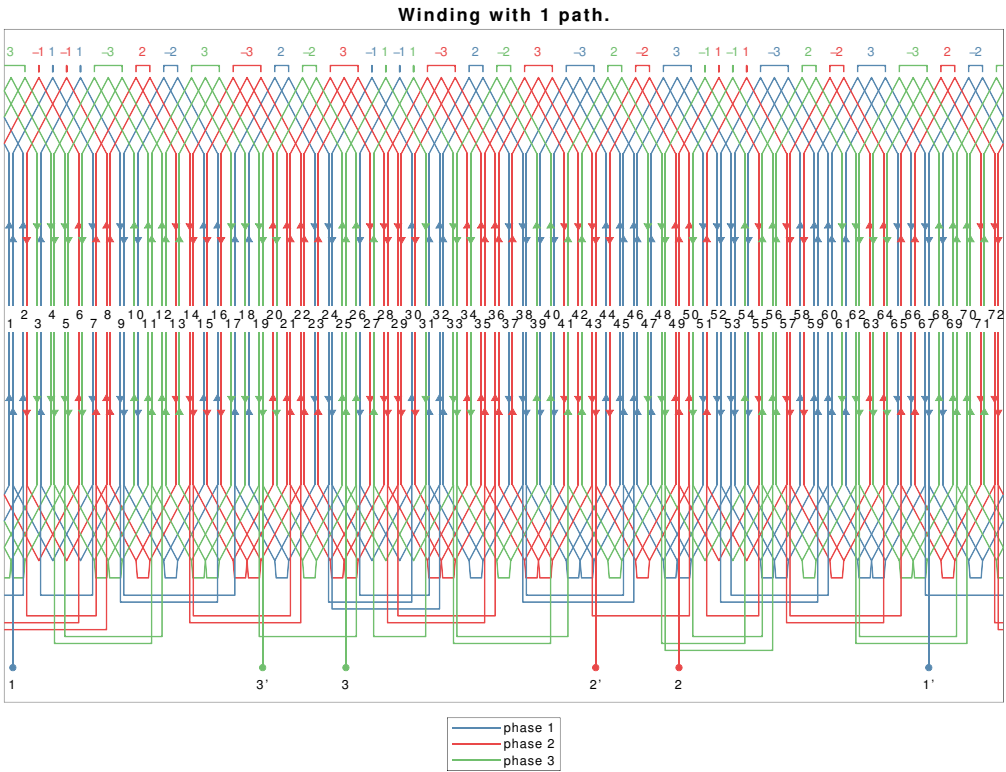


Figure 18. Winding scheme with a 3rd order single-sided imbrication for $N = 72$, $p = 5$ and $m = 3$.

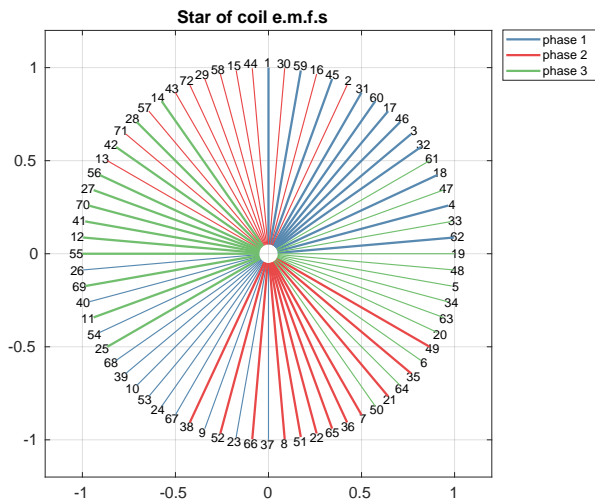


Figure 19. Double chording with a 3rd-order double-sided imbrication for $N = 72$, $p = 5$ and $m = 3$.

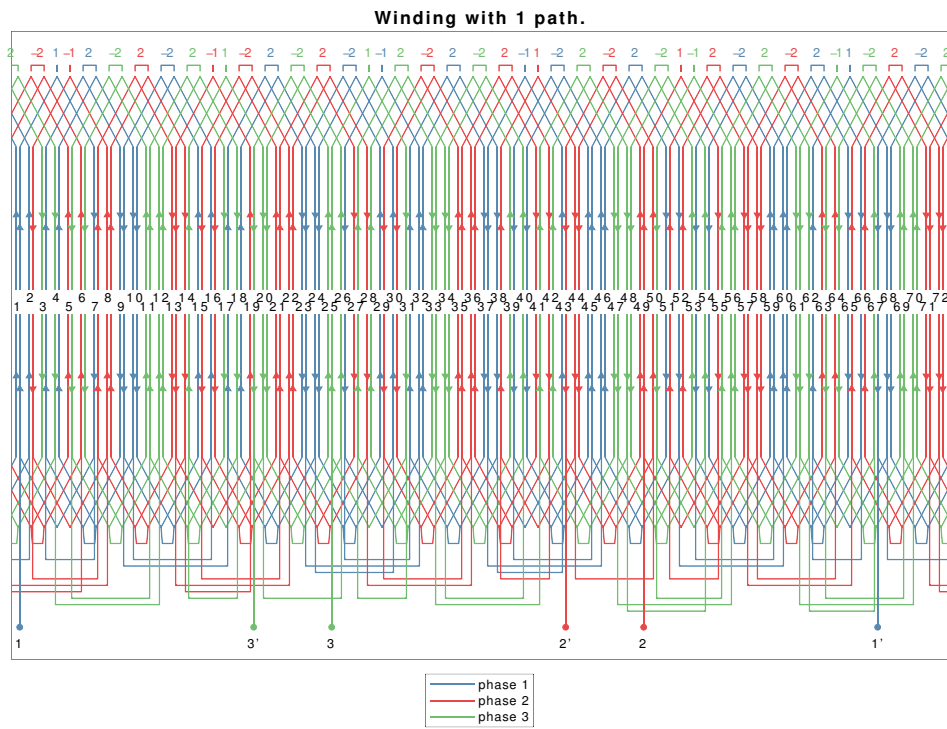


Figure 20. Winding scheme with a 3rd order double-sided imbrication for $N = 72$, $p = 5$ and $m = 3$.

Table 18. Triple chording with a 3-rd order double-sided imbrication and zone widening by 2 coils for $N = 72, p = 5$ and $m = 3$

1	-54	59	-40	45	-26	31	60	17	46	3	32	61	18	-23	4	-9	62	-67	48	-53	-10	-39	-68
49	-30	35	-16	21	-2	7	36	65	22	51	8	37	66	-71	52	-57	38	-43	24	-29	-58	-15	-44
25	-6	11	-64	69	-50	55	12	41	71	27	56	13	42	-47	28	-33	14	-19	72	-5	-34	-63	-20
	↑		↑		↑										↑		↑		↑				

(ph1: blue, ph2: red, ph3: green)

Table 19. Winding factor harmonics with different optimization techniques for $N = 72, p = 5$ and $m = 3$

Harm. order	Normal chording		Double chording		Triple chording
	WDT ($y_c = 7$)	Chording ($y_c = 6$)	1-sided imbric.	2-sided imbric.	2-sided imbric. + zone widen.
1-st	0.955	0.923	0.902	0.881	0.878
3-rd	0.633	0.451	0.365	0.277	0.268
5-th	0.201	0.154	0.026	0.002	0.002
7-th	0.132	0.036	0.008	0.020	0.017
9-th	0.201	0.154	0.013	0.154	0.109
11-th	0.080	0.087	0.078	0.072	0.055

3. the double sided imbrication is made by shifting upwards by two cells the 2-nd, the 4-th and the 6-th negative columns.

Finally, Table 19 summarizes the winding factor harmonics for each of the proposed optimization technique. It can be noticed that the chording allows a significant reduction of both the fifth and the seventh order harmonics, which are almost canceled by applying a double chording technique.

Similar results can be appreciated from Table 20, which summarizes the winding harmonic factors for different optimization techniques for a single-phase, double-layer winding located into 60 slots and with one pole pair. The corresponding WDT for the proposed example is plotted in Table 21. The modified WDT for a double chording with a 2-nd order double-sided imbrication is represented in Table 22. It can be noticed that, in case of imbrication, the WDT follows the same rules of the previous example shown in Table 17 and the corresponding star of slots and winding scheme are plotted in Figures 21 and 22, respectively.

The imbrication procedure can now be generalized.

1. For normal or non-reduced system windings the columns of positive slots that are to be shifted are shifted upwards by

$$s_{pos} = \begin{cases} \frac{m+1}{2} & \text{if } m \in \mathbb{U} \\ \frac{m}{2} & \text{if } m \in \mathbb{G} \end{cases} \tag{25}$$

Table 20. Winding factor harmonics with different optimization techniques for $N = 60, p = 1$ and $m = 1$

Harmonic order	WDT ($y_c = 30$)	Chording ($y_c = 24$)	Single-sided imbrication	Double-sided imbrication
1-st	0.827	0.787	0.778	0.761
3-rd	0	0	0	0
5-th	0.167	0	0	0
7-th	0.121	0.071	0.035	0.20
9-th	0	0	0	0
11-th	0.080	0.076	0.014	0.087

Table 21. WDT with a double chording and a 3-rd order double-sided imbrication for $N = 60, p = 1$ and $m = 1$

1	2	3	4	5	6	7	8	9	10	-11	-12	-13	-14	-15	-16	-17	-18	-19	-20
21	22	23	24	25	26	27	28	29	30	-31	-32	-33	-34	-35	-36	-37	-38	-39	-40
41	42	43	44	45	46	47	48	49	50	-51	-52	-53	-54	-55	-56	-57	-58	-59	-60

Table 22. WDT with a double chording and a 3-rd order double-sided imbrication for $N = 60, p = 1$ and $m = 1$

1	-42	3	-44	5	6	7	8	9	10	-31	12	-33	14	-35	-36	-37	-38	-39	-40
21	22	23	24	25	26	27	28	29	30	51	32	53	34	55	56	57	58	59	60
41	-22	43	-24	45	46	47	48	49	50	-11	52	-13	54	-15	-16	-17	-18	-19	-20
	↑		↑								↑		↑						

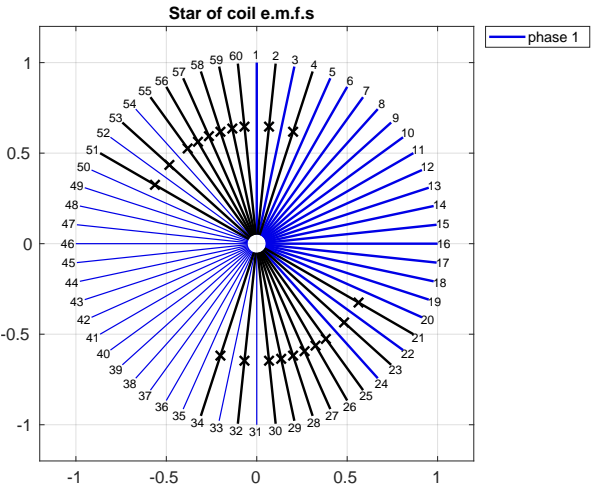


Figure 21. Double chording with a 2nd order double-sided imbrication for $N = 60, p = 1$ and $m = 1$.

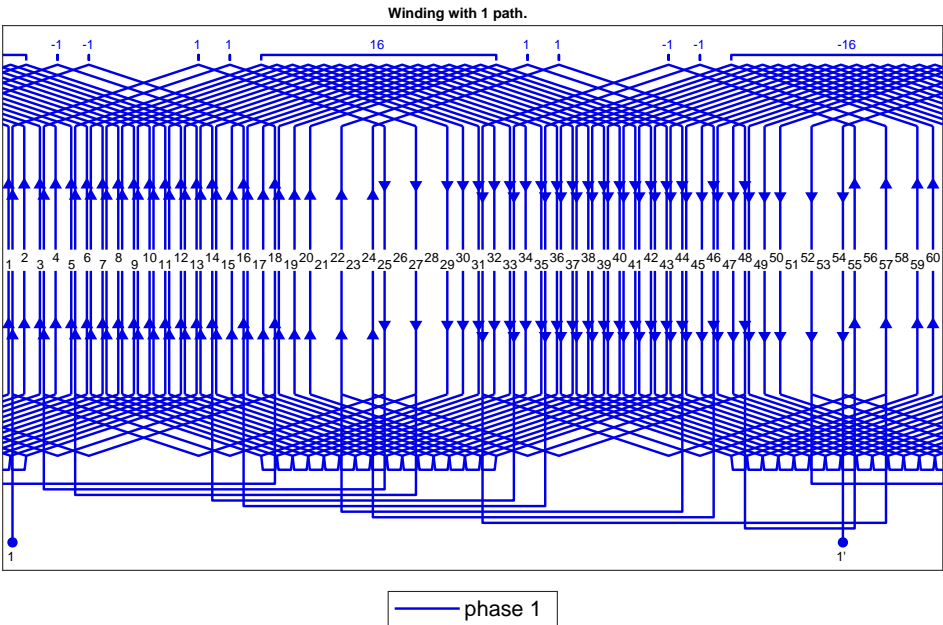


Figure 22. Winding scheme with a 2nd order double-sided imbrication for $N = 60, p = 1$ and $m = 1$.

Table 23. WDT of a 6-phase reduced winding with $N = 96$, $p = 5$, $q = 1 + 2/10$.

1	30	59	16	45	2	31	60	17	46	3	32
61	18	47	4	33	62	19	48	5	34	63	20
49	6	35	64	21	50	7	36	65	22	51	8
37	66	23	52	9	38	67	24	53	10	39	68
25	54	11	40	69	26	55	12	41	70	27	56
13	42	71	28	57	14	43	72	29	58	15	44

Table 24. WDT of a 6-phase reduced winding with $N = 96$, $p = 5$, $q = 1 + 2/10$, after swapping.

1	30	59	16	45	2	-37	-66	-23	-52	-9	-38
31	60	17	46	3	32	-67	-24	-53	-10	-39	-68
61	18	47	4	33	62	-25	-54	-11	-40	-69	-26
19	48	5	34	63	20	-55	-12	-41	-70	-27	-56
49	6	35	64	21	50	-13	-42	-71	-28	-57	-14
7	36	65	22	51	8	-43	-72	-29	-58	-15	-44

(ph1: blue, ph2: green, ph3: red, ph4: cyan, ph5: magenta, ph6: yellow)

cells, whereas the columns of negative slots must be shifted upwards by

$$s_{neg} = \begin{cases} \frac{m+1}{2} & \text{if } m \in \mathbb{U} \\ \frac{m+2}{2} & \text{if } m \in \mathbb{G} \end{cases} \quad (26)$$

- For reduced system windings both the positive and the negative columns are to be shifted always upwards by 1 cell, i.e.

$$s_{pos} = 1 \text{ and } s_{neg} = 1 \quad (27)$$

The sign of the cells of the last row must be then changed.

To clarify the procedure to carry out an imbrication in a reduced winding the following example is presented. Here a 6-phase reduced winding with $N = 96$, $p = 5$, $q = 1 + 2/10$ is considered.

After swapping Quadrants 1 and 3 of Table 23 and reordering it following Table 6 we obtain Table 24.

Now, by shifting upwards both columns 2 and 8 by one cell ($s_{pos} = 1$ and $s_{neg} = 1$), and by changing the signs of the cells in the last row of the shifted columns (here row nr. 6) we obtain, finally, Table 25. Here again, in order to realize a radial symmetrical system, the even phase groups must be multiplied by -1 (i.e. rows 3 and 4 in Table 25).

The star of slots of the winding configuration without imbrication is shown in Figure 23a, whereas the final configuration is shown in Figure 23a. $N = 96$, $p = 5$, $m = 6$ and $q = 1 + 2/10$.

Table 25. WDT of a 6-phase reduced winding with $N = 96$, $p = 5$, $q = 1 + 2/10$, and double sided imbrication of the 1-st order.

1	60	59	16	45	2	-37	-24	-23	-52	-9	-38
31	18	17	46	3	32	-67	-54	-53	-10	-39	-68
61	48	47	4	33	62	-25	-12	-11	-40	-69	-26
19	6	5	34	63	20	-55	-42	-41	-70	-27	-56
49	36	35	64	21	50	-13	-72	-71	-28	-57	-14
7	-30	65	22	51	8	-43	66	-29	-58	-15	-44

(ph1: blue, ph2: green, ph3: red, ph4: cyan, ph5: magenta, ph6: yellow)

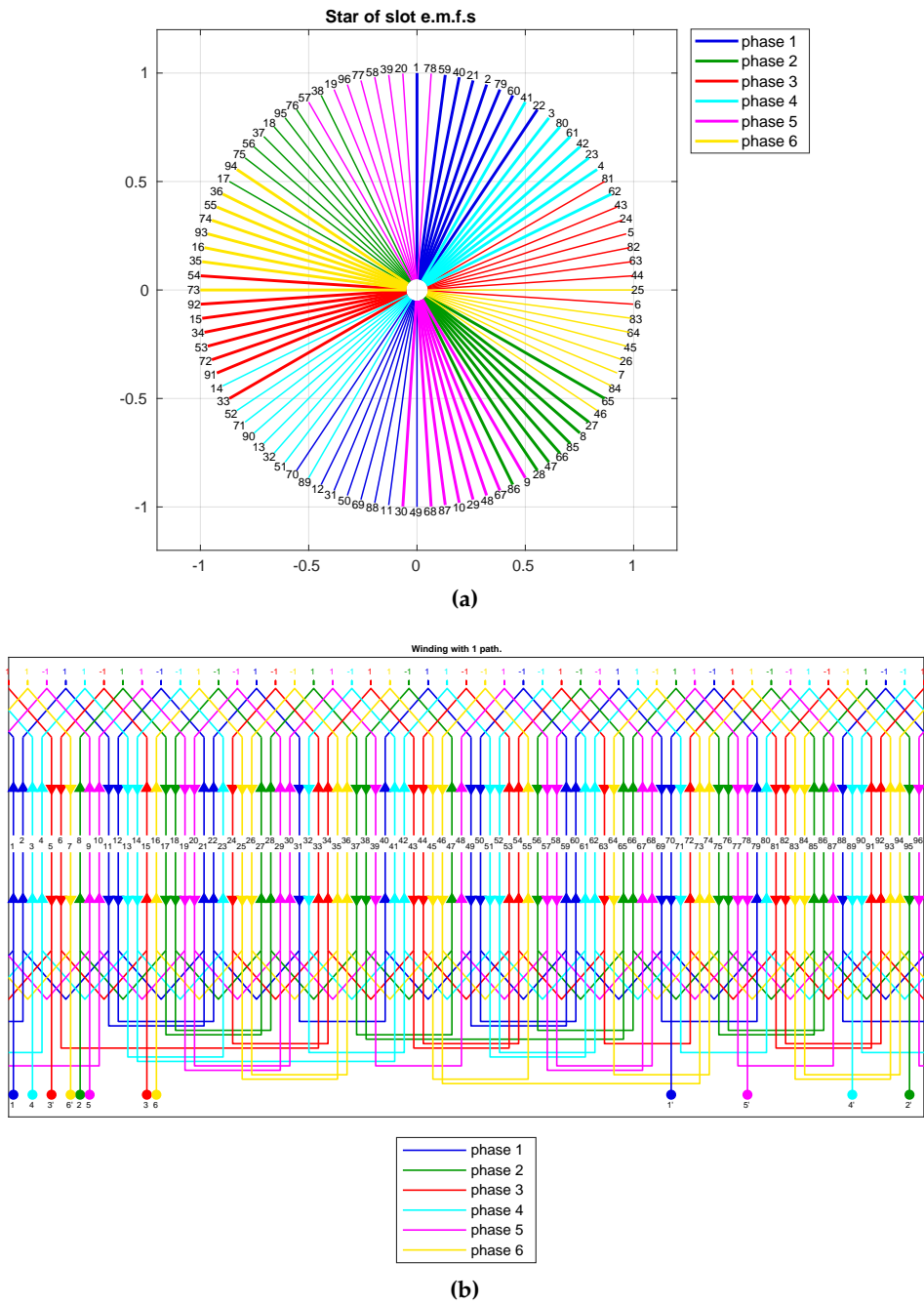


Figure 23. (a) Star of slots of a 6-phase reduced single-layer winding with $N = 96$, $p = 5$ and (b) related winding scheme with 1-st order imbrication.

5. Conclusions

This paper has presented a new, simple and effective procedure for the determination of the EMF stars distribution and the winding configuration in all possible typologies of electrical machines equipped with symmetrical windings by means of the WDT. The main advantage of the WDT consists in its very simple construction and interpretation, which simplifies also the determination of the winding characteristics in terms of harmonic content. With this method the construction of star of slots is no longer needed even if in this paper they have been shown but only for clarity's sake. Furthermore, as reported in the various examples, WDT can be applied to all type of windings, allowing the resolution of complex problems by adopting only 3 fundamental rules. Winding optimization procedures, such as double chording, interspersing (single or double-sided) and zone widening or shortening can be easily implemented with simple and general standard procedures and can be applied to all type of windings derived by both reduced and normal systems. Moreover, the WDT is easy to be implemented on a computer and it can, therefore, be considered as a very useful tool particularly within the phase of rapid winding design. The winding examples proposed in this work include symmetrical windings with integer and fractional slot numbers both normal and reduced (radial symmetrical windings). The examples shown successfully validate the WDT procedure.

References

1. Arnold, E. *Die Ankerwicklungen und Ankerkonstruktionen der Gleichstrom-Dynamomaschinen*, 3 ed.; Springer: Berlin, München, Germany, 1899.
2. Arnold, E. *Die Wicklungen der Wechselstrommaschinen*, 2 ed.; Vol. 3, *Die Wechselstromtechnik*, Verlag von Julius Springer: Berlin, Germany, 1912.
3. Richter, R. *Ankerwicklungen für Gleich- und Wechselstrommaschinen: Ein Lehrbuch*; Springer Verlag: Berlin-Heidelberg, Germany, 1920.
4. Kauders, W. Systematik der Drehstromwicklungen. II. Teil. *Elektrotechnik un Maschinenbau* **1934**, 52, 85.
5. Heller, F.; Kauders, W. Das Görgessche Durchflutungspolygon. *Archiv für Elektrotechnik* **1935**, 29, 599–616.
6. Richter, R. *Lehrbuch der Wicklungen elektrischer Maschinen*; Wissenschaftliche Bücherei, Verlag und Druck G. Braun: Karlsruhe, Germany, 1952.
7. Sequenz, H. *Die Wicklungen elektrischer Maschinen: Wechselstrom Ankerwicklungen.*; Vol. 1, Springer Verlag: Wien, Austria, 1950.
8. Sequenz, H. *Die Wicklungen elektrischer Maschinen: Wenderwicklungen*; Vol. 2, Springer Verlag: Wien, Austria, 1952.
9. Sequenz, H. *Die Wicklungen elektrischer Maschinen: Wechselstrom-Sonderwicklungen*; Vol. 3, Springer Verlag: Wien, Austria, 1954.
10. de Pistoye, H. Bobinages à courant alternatif à trous partiels. *Revue générale de l'Electricité* **1923**, 14, 798.
11. Heller, B.; Hamata, V. *Harmonic field effects in induction machines*; Elsevier Scientific Pub. Co., 1977.
12. Rebora, G. Avvolgimenti trifase. *Elettrotecnica* **1931**, 618, 72.
13. Seike, T. Die einfache Ausführung der Bruchloch-Ankerwicklungen für Wechselstrom. *Elektrotechnik un Maschinenbau* **1931**, 49, 21.
14. Liwischitz-Garik, M.; Gentilini, C. *Winding alternating-current machines: a book for winders, repairmen, and designers of electric machines*; Van Nostrand: New York, USA, 1950.
15. Liwischitz, M.M. Balanced fractional-slot wave windings. *Electrical Engineering* **1948**, 67, 893–893.
16. Liwischitz, M.M. Doubly chorded fractional-slot windings. *Electrical Engineering* **1948**, 67, 848–848.
17. Malti, M.G.; Herzog, F. Fractional-slot and dead-coil windings. *Electrical Engineering* **1940**, 59, 782–794.
18. Hellmund, R.; Veinott, C. Irregular windings in wound rotor induction motors. *Electrical Engineering* **1934**, 53, 342–346.
19. Tingley, E.M. Two- and Three-Phase Lap Windings in unequal Groups. *The Electrical Review and Western Electrician* **1915**, 66, 166–168.
20. A. O. Di Tommaso.; Genduso, F.; Miceli, R. A New Software Tool for Design, Optimization, and Complete Analysis of Rotating Electrical Machines Windings. *IEEE Transactions on Magnetism* **2015**, 51, 1–10.

21. Smith, A.; Delgado, D. Automated AC Winding Design. 5th IET International Conference on Power Electronics, Machines and Drives (PEMD 2010), 2010, pp. 1–6.
22. Steinbrink, J. Design and Analysis of Windings of Electrical Machines. International Symposium on Power Electronics, Electrical Drives, Automation and Motion, 2008. SPEEDAM 2008, 2008, pp. 717–720.
23. Bianchi, N.; Pre, M.D. Use of the star of slots in designing fractional-slot single-layer synchronous motors. *IEEE Proceedings - Electric Power Applications* **2006**, *153*, 459–466.
24. Wach, P. Algorithmic method of design and analysis of fractional-slot windings of AC machines. *Electrical Engineering* **1998**, *81*, 163–170.
25. Huth, G. Optimierung des Wicklungssystems bei permanentmagneterregten AC - Servomotoren. *Electrical Engineering* **1999**, *8*, 375–383.
26. A. O. Di Tommaso.; Genduso, F.; Miceli, R.; Galluzzo, G.R. An Exact Method for the Determination of Differential Leakage Factors in Electrical Machines With Non-Symmetrical Windings. *IEEE Transactions on Magnetics* **2016**, *52*, 1–9.
27. Germishuizen, J.J.; Kamper, M.J. Classification of symmetrical non-overlapping three-phase windings. The XIX International Conference on Electrical Machines - ICEM 2010, 2010, pp. 1–6.
28. Pyrhonen, J.; Jokinen, T.; Hrabovcová, V. *Design of rotating electrical machines*; John Wiley & Sons: New Delhi, India, 2009.
29. Heiles, F. *Wicklungen elektrischer Maschinen und ihre Herstellung*, 2 ed.; Springer: Berlin, Göttingen, Heidelberg, 1953; p. 270.
30. Müller, G.; Vogt, K.; Ponick, B. *Berechnung elektrischer Maschinen*, 6 ed.; Elektrische Maschinen, Wiley-VCH Verlag GmbH & Co KGaA: Weinheim, Germany, 2008.
31. Huth, G. Eigenschaften strangverschachtelter Einschichtwicklungen für Drehstrom-Asynchronmotoren. *Electrical Engineering* **1997**, *80*, 369–373.